PRESS FORMING THE DOUBLE-DOME BENCHMARK GEOMETRY USING A 0/90 UNIAXIAL CROSS-PLY ADVANCED THERMOPLASTIC COMPOSITE

P. Harrison[1*], R. Gomes[2], N. Correia[2], F. Abdiwi[1], W.R. Yu[3]

[1]*School of Engineering, James Watt Building (South) University of Glasgow, Glasgow, G12 8QQ, UK*
[2]*INEGI, Composite Materials and Structures Research, Institute of Mechanical Engineering and Industrial Management, Porto 4200-465, Portugal*
[3]*Department of Materials Science and Engineering, Seoul National University, Seoul 151-742, Korea*
**Philip.harrison@glasgow.ac.uk*

Keywords: thermoforming, cross-ply composite, finite element simulations

Abstract
A pre-consolidated thermoplastic advanced composite cross-ply sheet comprised of two uniaxial plies orientated at 0/90^o has been thermoformed using tooling based on the double-dome bench-mark geometry. The shear behavior of the material has been characterised as a function of rate and temperature using the picture frame test technique. Multi-scale modelling predictions of the material's shear behavior, based on the fibre volume fraction, approximate matrix rheology and measured meso-scale kinematics, have been made and incorporated in the forming predictions. Thermoforming experiments have been simulated using the finite element method, predictions are compared against the experimental results.

1 Introduction
The aim of this work is to investigate the thermo-forming of cross-ply laminates and to examine the utility of a predictive, micro to macro modelling strategy in simulating the forming operation. The suitability of biaxial constitutive models, originally designed to model the shear behavior of textile composites and engineering fabrics, to predict the forming behavior of uniaxial cross-ply laminate is assessed.

2 Material
Pre-consolidated uniaxial cross-ply sheet, approximately 0.7mm thick, comprised of two layers of unidirectional glass-polypropylene plies, with a 0/90 initial fibre orientation has been used. The composite consists of a polypropylene homo-polymer matrix containing of 60% volume fraction E-glass fibres (consisting of two consolidated layers of Polystrand ThermoPro Standard 60% 10 series [1], as supplied by the manufacturer).

3 Experimental set-up for high temperature press-forming of double-dome
The double-dome bench mark geometry [2] has been manufactured at INEGI as a set of matched male and female steel tools (see Figure 1). The geometry was chosen to allow comparison of the results found in this investigation, using this molten pre-consolidated cross-ply composite with results found by other investigators who used engineering fabrics [e.g. 3-6] and also to provide experimental data for evaluation of constitutive models designed for

thermoplastic materials. The experimental set-up used here is close to that of the benchmark set-up, though certain features have been changed to facilitate forming at high temperature. In particular, the blank-holder boundary conditions and the initial blank shape have been modified.

3.1 Manufacture of Double Dome tooling

CAD model for the double-dome were downloaded from [2]. The models were exported from Solidworks to CAM software (PowerMILL, Delcam) and machining was performed on a 5-axis CNC machine (Fadal, VMC 4020). The tools were fitted with heating cartridges in top and bottom tools with cooling facility in just the bottom tool, though in this investigation room temperature tooling was used in all tests.

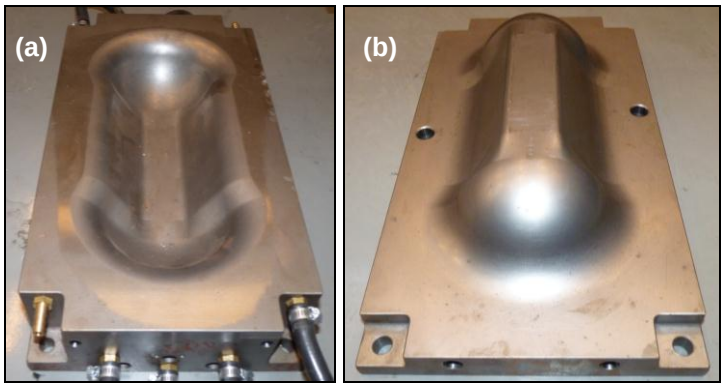

Figure 1. Tooling based on CAD model from [2]. (a) Female die (b) Male punch.

3.2 Heating and transfer system

In order to form the pre-consolidated uniaxial cross-ply sheet the polymer matrix had to be heated to above its melt-temperature and quickly transferred to the press for forming. An open-sided radiant heater oven (see Figure 2) was designed together with a compressed-air driven shuttle system, to enable fast transfer from oven to press. The heater contained eight 1kW radiant heating lamps (Elstein, FSR 1000-230V), situated inside the top and bottom of the oven (Figure 2a) and the blank sheet was automatically positioned between the two heaters using a blank-holder frame and shuttle rails (see Figure 2b).

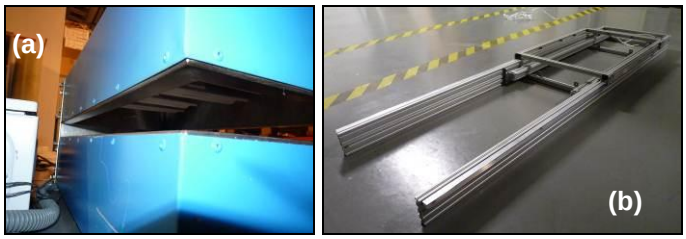

Figure 2. (a) Radiant heater used to heat blank. The upper heating lamps are visible, similar lamps are also positioned in the bottom of the oven. (b) Shuttle system frame and blank-holder frame.

After various experiments, the most controllable method of heating the sheet was found to involve pre-heating the oven to a set temperature with a metal partition sheet separating the top and bottom halves of the oven. Equilibrium was achieved in both regions after approximately 5 to 10 minutes. The heaters were switched off before removing the metal partition sheet and the composite blank was inserted. A 260^{o}C pre-heat temperature produced the heating profile within the blank shown in Figure 3a (measured using a specially designed temperature probe involving a thermocouple sandwiched inside 2 uniaxial consolidated sheets). The blank was removed from the oven after 100s, when the rate of change of

temperature of the blank was lowest (see Figure 3a). This enabled better control of the blank temperature prior to forming. The subsequent cooling rate (see Figure 3b) of the blank when removed from the oven was measured as approximately linear at -2.96 +/- 0.31$^{o}Cs^{-1}$ (error indicated using standard deviation). The average shuttle transfer time was measured at 0.73 +/- 0.06s. The average press closure time was measured at 2.68s +/- 0.19s. Thus, the total time from removing the sheet from the oven to press closure was about 3.4 +/- 0.25s. Four experiments were conducted using an oven temperature set to 260^{o}C and an estimated blank forming temperature of between 186 to 218^{o}C. One further experiment was conducted using an oven temperature was set to 270^{o}C and an estimated blank forming temperature of between 196 to 228^{o}C. The oven temperature and fibre orientation for these experiments is given in cases 1 to 5 of Table 1.

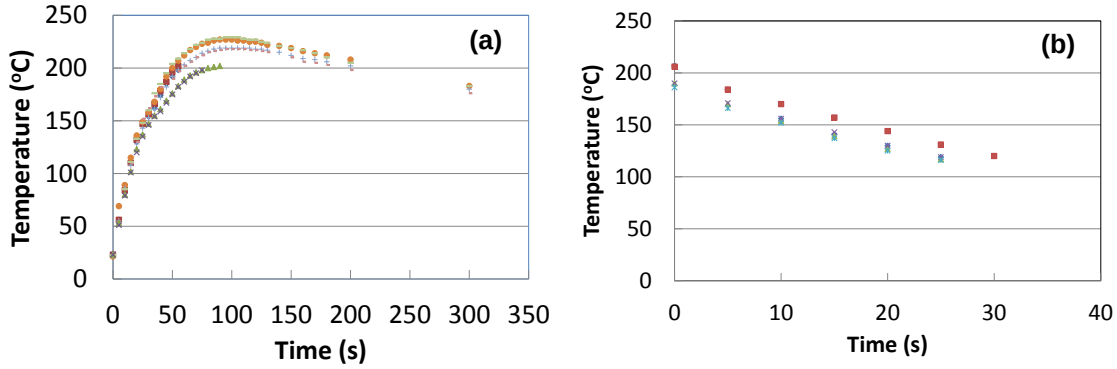

Figure 3. (a) Temperature profile of blank when placed in pre-heated oven (6 repeat tests) (b) cooling rate of blank when removed from the oven (5 repeat tests).

Case Number	Oven Temperature (^{o}C)	Fibre orientation (^{o})
1	260	0/90
2	260	0/90
3	260	+/- 45
4	270	+/- 45
5	260	-35/+55

Table 1. Oven temperature and initial blank orientations for the 5 formed parts.

3.3 Blank-holder system, blank shape and spring stiffness

The original set-up for the bench-mark experiment involves an arrangement in which the blank is constrained using a normal pressure applied to its surface using a segmented blank holder, as described in [2-6]. The set-up is difficult to use at high temperatures due to the need to heat the entire pre-consolidated thermoplastic blank prior to forming. The problem can be avoided using an alternative technique; applying tension via the use springs and clips, see Figure 4. The blank shape had to be modified from the bench-mark prescribed geometry of 270 x 470 mm [e.g. 4] for two reasons: (i) During forming of the sheet, clips attached to the blank are drawn towards the tooling. If the blank is too small the clips move between the tools and are crushed as the tools close. Thus, the clips had to be a minimum distance away from the tooling at the start of the test. (ii) In order for the blank-holder frame to fit inside the oven the latter had to employ an open-sided design (see Figure 2a). Material towards the outer edges of the oven experienced a slightly lower temperature compared to that at the centre of the oven. To minimise this effect, it was preferable to decrease the size of the blank. These two constraints suggested an optimum shape for the blank involving tabs, as shown in Figure 5a. By transferring the entire sheet and clips into a radiant oven for heating, only small areas of the sheet (the tabs held between the clips) remain un-melted. Springs were cut from a long

section of coiled wired. Looped ends were made by bending the last two coils of the cut spring for attachment to bolt heads which protruded from the blank-holder frame (see Figure 4c). Two different lengths were made, involving either 19 to 20 or 25 to 26 turns in the main body section. Longer springs were used at the ends of the blank, shorter springs at the side in order to produce similar strains in the springs during forming. The stiffness and yield force of the springs were measured for each spring length, given in Table 2 together with the standard deviation of each result (from 3 tests).

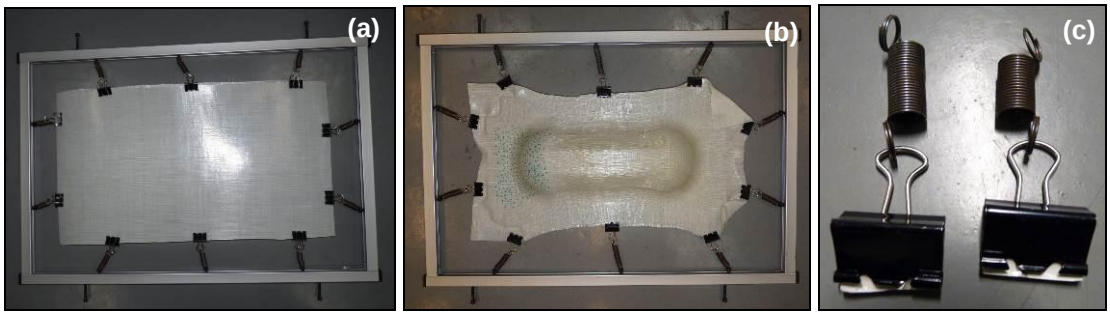

Figure 4. Preliminary testing using springs and clips to apply tension, a different sheet perimeter was chosen for the final experiments. (a) sheet before forming (b) sheet after forming (c) Two types of spring used to induce tension in blank during forming. Longer springs (25-26 turns) were use at the ends, shorter springs (19-20 turns) were used at the sides of the blank. Sand paper was glued inside the clips to prevent slip.

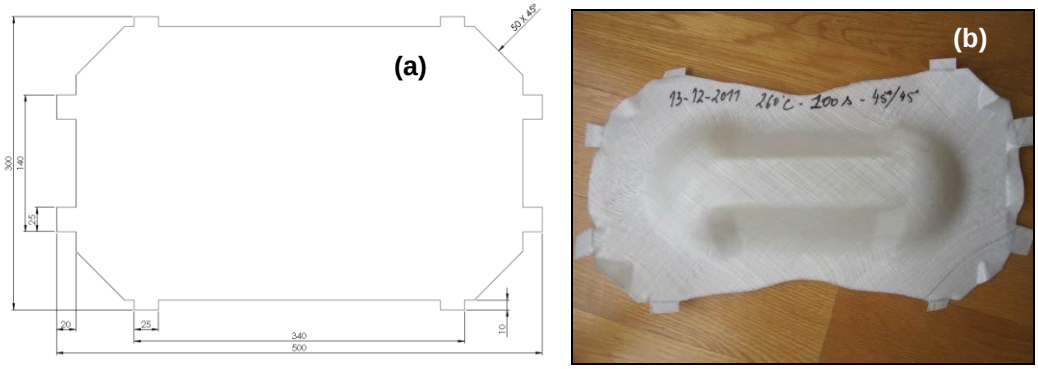

Figure 5. (a) Dimensions of blank use in forming experiments (in mm). (b) Formed part using final perimeter shape, the tabs used to hold the sheet using the clips are clearly visible.

Spring	Stiffness (N/mm)		Yield load (N)	
	Average	S.D.	Average	S.D.
Long	0.210	0.010	3.38	3.47
Short	0.277	0.009	5.71	3.65

Table 2. Stiffness and yield load of springs (average value plus standard deviation**)**

4 Shear Force Characterisation and Prediction for UD cross-ply sheet

4.1 Picture frame shear characterisation

The shear response of the composite has been characterised as a function of both rate and temperature, using the picture frame test method [7]. The side length of the picture frame rig used here is 170 mm (clamping length = 130 mm). In order to filter spurious results due to misalignment a strategy based on the following guidelines was used: (i) the result should be the lowest force curve produced under a given experimental state (rate, temperature), (ii) the result can only be used up until wrinkling of the specimen is observed during the test and (iii) the data should be physically consistent; the force versus shear angle curves should generally

increase with increasing shear rate (at a given temperature) and with decreasing temperature (at a given shear rate). This technique was used in producing the data shown in Figure 6 which, for clarity, is presented using both (a) linear-linear and (b) log-linear axis.

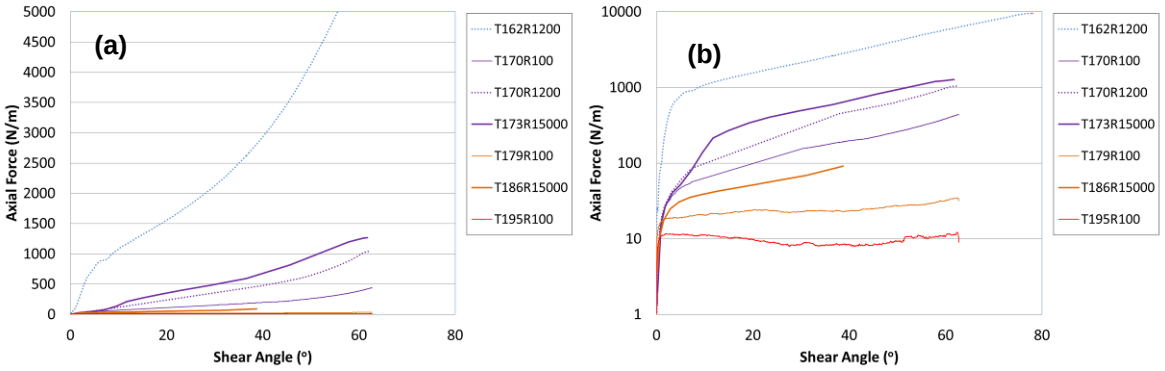

Figure 6. Normalised axial force versus shear angle results produced at various temperatures and cross-head displacement rates. For clarity, the same data are presented on (a) linear-linear and (b) log-linear axis.

A firmly clamped specimen boundary condition was used for all tests. Due to unavoidable misalignments, of the 35 tests that were conducted, only 7 were found to meet conditions (i) to (iii). The legend indicates the measured temperature in ^{o}C (thermocouple attached to the sample), and the crosshead displacement rate in mm/min, e.g. T162R1200 indicates a temperature of 162^{o}C and a rate of 1200 mm/min. The shear angle was determined from the cross-head displacement [7]. Friction in the picture frame rig was characterised and subtracted from the measured data (friction was a significant source of noise at the higher temperatures). Given the high discard rate of test data, a strategy to produce enough data with which to calibrate and evaluate shear force versus shear angle predictions (see Section 4.3) using a multi-scale energy model developed previously [8] has been adopted.

4.2 Meso-scale kinematics during shear

The meso-scale kinematics occurring during shear of advanced composites is a significant factor in determining the shear resistance of the material [8-12]. Two tests were conducted at both 160^{o}C and 190^{o}C, at a cross-head displacement rate of 100mm/min.

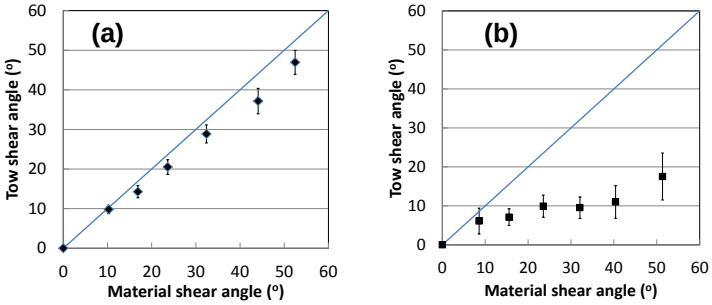

Figure 7. Average meso-scale tow shear kinematics occurring at (a) 165^{o}C and (b) 190^{o}C. The blue line indicates the kinematics corresponding to a continuous strain profile across the specimen

By marking ink lines across the surface of the samples prior to testing, both along and orthogonal to the fibre direction, the material shear angle and the shear strain profile across the samples could be analysed. *ImageJ* [13] was used to perform image analysis using digital photographs taken at different instances in time during the course of the tests. Similar observations of discontinuous meso-scale kinematics have been made previously on woven glass/molten polypropylene textile composite [8,11], stitched non-crimp fabrics [10], engineering fabrics [12] and uniaxial prepregs [9]. In this investigation, the degree of

discontinuity in the shear strain profile across the sheet has been found to depend strongly on temperature. Figure 7 shows the average tow shear angle versus the material shear angle for (a) 165°C and (b) 190°C. The average initial width of the tows was 2.21 +/- 0.63mm at 165°C and 2.10 +/- 0.41mm at 190°C.

4.3 Multi-scale energy model shear force predictions

Shear force versus shear angle input curves across a range of shear rates are required by the rate-dependent elastic constitutive model used to simulate viscous behavior during the forming simulations [14]. To provide this data a multi-scale energy model designed to predict the shear response of pre-impregnated (viscous) advanced composites from fabric architecture, fibre volume fraction and matrix rheology is employed [8]. Tow kinematics measured at the higher temperature in this investigation (see Figure 7b) have been quantified using a cubic polynomial and incorporated in the model. Parameters reflecting the fabric architecture have also been adjusted to suit a uniaxial cross-ply fabric (the weave factor *q* is set to 1 and the average tow width incorporated). The specific matrix rheology of the PP matrix in the composite used in this investigation has not yet been measured and so the Carreau-Yasuda rheological model and Arrenhius parameters fitted to a polypropylene characterised previously [8] have been used. The viscosity of different batches of PP can vary by several times at different rates and temperatures in a non-linear manner due to differences in molecular weight. Thus, the multi-scale energy model predictions have been multiplied by a constant scale factor to give an approximate match with shear force results from the picture frame test at a given temperature (black lines in Figure 8). The first reference result for the scaling has been chosen to be the T170R100 curve (see Figures 6 and 8) and a scale factor of 4.5 has been used to modify the multi-scale model predictions. Axial force predictions produced by finite element picture frame simulations using the Stress Power Model (SPM) incorporating the scaled multi-scale energy model predictions for both the reference test and the T170R1200 test are compared in Figure 8 (dashed grey lines). Predictions for a third cross-head displacement rate (T170R2600) are also included as these rates are close to those experienced by the composite during the forming experiments (estimated from finite element forming simulations and the average press forming time). A similar process was used to make predictions at 200°C at the same rates (see legend in Figure 8 – continuous grey lines), this time using the T195R100 test result as a guide (dotted black line). A constant scale factor of 0.05 was found to provide a reasonable match at this temperature. The scaled multi-scale model predictions for 200°C are used in the forming simulations reported in Section 3.

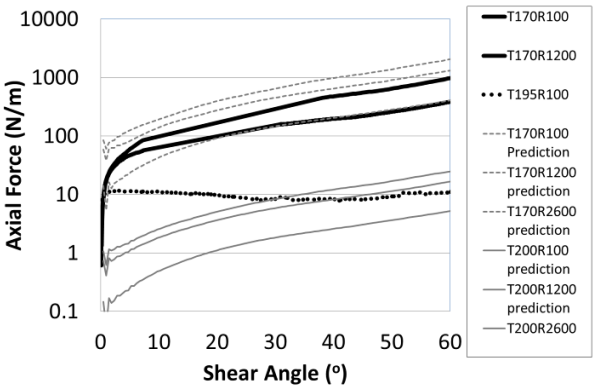

Figure 8. Multi-scale energy model predictions scaled to give a reasonable correspondence with experimental data.

3 Comparison of Experimental and Numerical Forming Simulations

The Stress Power Model (SPM) described in [14] and implemented in the commercial finite element code Abaqus Explicit™ has been used to simulate the forming process. This model

uses rate dependent elastic input curves to simulate viscous behavior at a given temperature (here 200°C) by incorporating predictions of the scaled multi-scale energy model as input. The interface between the multi-scale energy model predictions and the SPM is most effective when truss and membrane elements are employed to simulate the fibre and shear stiffnesses respectively. An in-house code, MeshGen, capable of automatically generating mixed truss and membrane meshes of arbitrary perimeter shape, has been used to generate the mesh for the blank, in this case using 63,078 truss (diameter = 0.02mm, modulus = 65×10^6 Pa) and 31,168 square membrane (thickness 0.7mm) elements of side length 2mm (similar to the mesh density used in [4]). The material density of all deformable elements was 375,000kgm^{-3}. Use of an artificially low modulus and high density decreased simulation times (approximately 2 hours using a 32 bit Windows OS with Intel Core i7-2720QM CPU @ 2.2 GHz and 4 GB RAM, future investigations will examine the sensitivity of shear angle predictions to these modifications). Non-linear spring elements with properties given in Table 2 were used to attach the blank to the blank-holder frame. The latter was simulated using rigid body elements. Tabs on the blank were simulated as fibre-reinforced un-molten PP with a matrix modulus of 0.2GPa and a yield stress of 400kPa. The ratio between internal strain energy and kinetic energy in the simulations was checked to ensure inertial effects were negligible. The friction coefficient between tools and blank was 0.1. An image of the 0/90 blank orientation simulation (minus the die and punch tools) is shown in Figure 9a at 85% of full tool closure, beyond this small wrinkles begin to occur within the forming sheet which cause erroneous shear angle predictions. Future work will involve use of suitably modified shell, rather than membrane element to stabilize the sheet. Referring to Figure 9b, points 1-10 are the measurement locations recommended for use in the benchmark forum [2] whereas points 11-20 are the locations used by Khan et al. [4] for the case of the 0/90 sheet orientation. In Figure 9b only the experimental data for cases 1 and 2 (see Table 1) are given at points 1-10. For points 11-20, experimental data from this investigation (again cases 1 and 2) are compared with those presented by Khan et al [4]. Results from that investigation were obtained using an engineering fabric employing a different boundary condition and blank perimeter shape to the current investigation and are therefore not expected to be identical to experimental results from this investigation. Nevertheless, they are included as they do make an interesting comparison.

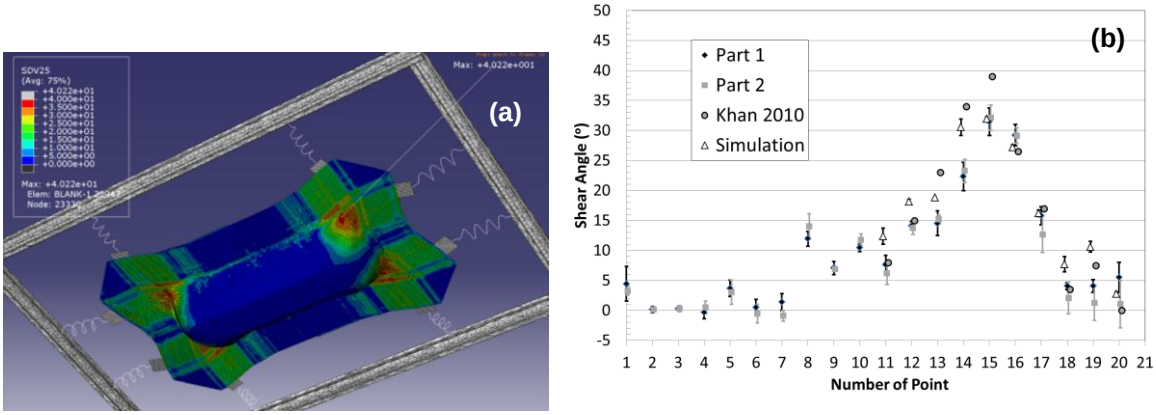

Figure 9. (a) FE forming simulation based on multi-scale model predictions. Colour legend indicates the shear angle. (b) Comparison between cases 1 and 2 (see table 1), simulation predictions (see Fig 9a) and the experimental results from Khan et al. [4].

Forming simulation predictions at 85% closure are also shown in Figure 9b for points 11-20. The comparison is reasonable though future work will aim to produce comparisons at 100% closure by employing a modified shell element formulation to incorporate a low but finite out-of-plane bending modulus. Further, the model will use a more realistic friction condition and

importantly, take account of the 'freezing' and the consequent sudden stiffening of the composite when coming into contact with the room-temperature tooling. The full set of experimental and numerical results will be presented in a subsequent publication.

Acknowledgements
The authors wish to thanks the Royal Academy of Engineering and the National Research Foundation (NRF) for sponsoring this research through the SRC/ERC program of MOST/KOSFE (R11-2005-065).

References

[1] http://www.polystrand.com/ProductsProcessing/ProductSeries/tabid/1003/Default.aspx (accessed 5th April 2012)
[2] http://www.wovencomposites.org/index.php Woven Composites Benchmark Forum, 2008 (accessed 4th May 2012)
[3] Willems, A., Lomov, S.V., Verpoest, I., Vandepitte, D., Harrison, P. and Yu, W.R. Forming simulation of a thermoplastic commingled woven textile on a double dome. *International Journal of Material Forming*, **1**, pp. 965-968, (2008)
[4] Khan, M.A. Khan, T. Mabrouki, E. Vidal-Sallé, P. Boisse, Numerical and experimental analyses of woven composite reinforcement forming using a hypoelastic behaviour. Application to the double dome benchmark. *Journal of Materials Processing Technology*, **210**, pp. 378–388, (2010)
[5] Lee, W., Um, M.-K., Byun, J.H., Boisse, P. and Cao, J. Numerical study on thermo-stamping of woven fabric composites based on double-dome stretch forming, *International Journal of Material Forming*, **3**(2), pp. S1217–S1227, (2010)
[6] Peng, X. and Rehman, Z.U. Textile composite double dome stamping simulation using a non-orthogonal constitutive model, *Composites Science and Technology*, **71**, pp. 1075–1081, (2011)
[7] Cao J., Akkerman R., Boisse P., et al. Characterization of Mechanical Behavior of Woven Fabrics: Experimental Methods and Benchmark Results, *Composites Part A*, **39**, 6, pp. 1037-1053, (2008)
[8] Harrison, P., Clifford, M.J., Long, A.C. and Rudd, C.D. A constituent-based predictive approach to modelling the rheology of viscous textile composites, *Composites: Part A*, **38**, 7-8, pp. 915-931, (2004)
[9] Potter, K., Bias extension measurements on cross-plied unidirectional prepreg *Composites Part A*, **33**, 63-73, (2002)
[10] Harrison, P., Wiggers, J., Long, A.C. and Rudd, C.D. *A constitutive model based on meso and micro kinematics for woven and stitched dry fabrics*, Proceedings of *14th International Conference on Composite Materials*, 14-18th July, San Diego, California, USA, (2003)
[11] Wang, J. *Predictive modelling and experimental measurement of composite forming behavior*, PhD thesis, University of Nottingham, (2008)
[12] Boisse, P., Meso-macro approach for composites forming simulation, *J Mater Sci*, **41**, pp. 6591–6598, (2006)
[13] http://rsbweb.nih.gov/ij/ (accessed 5th April 2012)
[14] Harrison, P., Yu, W.R. and Long, A.C. Rate Dependent Modelling of the Forming of Viscous Textile Composites, *Composites: Part A*, **42**, pp. 1719-1726, (2011)